Synergistic Regulation Effect of Magnesium and Acetate Ions on Structure Rigidity for Efficient and Robust $CsPbI_3$ Perovskite toward Red Light-Emitting Devices

*Xiufeng Wu,[a] Jiwei Wang,[a] Chengyuan Tang,[b] Lifang Li,[b] Wenda Chen,[b] Zhennan Wu,[b] Tingting Li,[*c] Hongwei Song,[*b] and Xue Bai[*b]*

[a] College of Physics, Liaoning University, Shenyang, China

[b] State Key Laboratory of Integrated Optoelectronics, College of Electronic Science and Engineering, Jilin University, 2699 Qianjin Street, Changchun 130012, China.

[c] School of Materials Science and Engineering, Jilin Jianzhu University, Changchun, China

[*] E-mail: litingting@jlju.edu.cn, songhw@jlu.edu.cn, baix@jlu.edu.cn

1. Experimental

1.1 Materials

Cs_2CO_3 (99.9%), PbI_2 (99.9%), $Mg(AcO)_2$·(98%), ODE (90%), OLA (80-90%) and OA (90%) were purchased from Aladdin and all were used directly.

1.2 Synthesis of the Cs-oleate solution

0.4 g Cs_2CO_3, 1 mL OA and 10 mL ODE were added into a 50 mL three-necked flask, then heated to 120 ℃ until the solution all dissolved and sustained at 100 ℃ for subsequent experiments.

1.3 Synthesis of $CsPbI_3$ NCs

For the synthesis of the pristine $CsPbI_3$ NCs, added 0.37 mmol PbI_2 (0.172 g), OA (1.5 ml) and ODE (15 ml) into a 50 mL 3-necked round-bottom flask and degassed under N_2 for 30 mins at 120 ℃, then injected 1.5 mL OLA and kept for 50 mins. Then, rapidly inject 0.8 mL of the prepared cesium oleate solution as the tempreture increase to 170 ℃. After 10 s, cool the reaction mixture in an ice water bath. The obtained product was separated by centrifugation for 10 mins at 9800 rpm and redispersed in 1.5 mL of cycloethane.

For the synthesis of $Mg(AcO)_2$ modified $CsPbI_3$ NCs, varied amounts of $Mg(AcO)_2$ (0.08, 0.16 and 0.25 mmol) and 0.37 mmol PbI_2 (0.172 g) were introduced to the 3-necked bottle together. And when the feeding amount is 0.30 mmol, the $CsPbI_3$ NCs was formed. The following steps are really analogous to the synthesis of the pristine $CsPbI_3$ perovskite NCs.

2. Characterizations and device Fabrication

2.1 Morphology and structure characterization

The XRD characterization of the samples were measured by a Rigaku D/Max-Ra X-ray diffractometer. And the TEM images and element mapping were imaged by a Titan transmission electron microscope (FEI Company) worked at 300 kV in EFTEM mode with a 20 KeV energy. The Inductively coupled plasma mass-spectrometry (ICP-MS) was measured on a Varian 720-ES ICP-optical emission spectrometer. X-ray photoelectron spectroscopy (XPS) patterns were obtained through a Kratos Axis Ultra DLD spectrometer equipped with a monochromatic Al K α X-ray source. The infrared Fourier spectroscopy was measured by a Fourier transform infrared (FT-IR) spectrometer from Japan with a mercury cadmium telluride detector. The AFM images were obtained by conducting a DI Innova AFM (Bruker) in light tapping mode.

2.2 Optical characterization

Optical studies. The UV-vis absorption spectra were obtained by the Shimadzu UV-3101PC UV-Vis scanning spectrophotometer. And the photoluminescence spectra were acquired by an FLS365 spectrometer. In addition, the absoluted quantum yield was then calculated by using the Edinburgh L920 software package. And the luminescence decay curves were measured by an FLS920 spectrofluorometer.

2.3 Device Fabrication and characterization

LED Fabrication. Indium tin oxide (ITO) substrates were cleaned by immersing in ethanol and acetone with ultrasonic agitation and then by UV-ozone treatment for 10

mins. A solution of ZnO NCs (50 mg mL^{-1}) was spin-coated onto the ITO glass at 1000 rpm for 30 s and annealed in air at 200 °C for 10 mins. Then, the substrate was transferred into a glovebox. A solution of polyethyleneimine (PEI) (dissolve in 2-methoxyethanol, 0.2% mass ratio) was spin coated onto the ZnO film at a speed of 3000 rpm and annealed at 125 °C for 10 mins. PNC active layers (20 mg mL^{-1}) were spin cast from toluene dispersions at 1000 rpm. 4,4′,4″-tris(carbazol-9-yl)-triphenylamine (TCTA), MoO_3 and Ag were then sequentially deposited by thermal evaporation in a vacuum deposition chamber (1×10^{-7} Torr).

Capacitor-like Device Fabrication. The capacitor-like devices were fabricated by spinning $CsPbI_3$ perovskite (20 mg mL^{-1}) at 1000 rpm for 40 s and depositing Ag by thermal evaporation in a vacuum deposition chamber.

Electron-only Device Fabrication. Cleaned ITO substrates were treated by UV-ozone for 10 mins. A solution of ZnO NCs (50 mg mL^{-1}) was spin-coated onto the ITO glass at 1000 rpm for 30 s and annealed in air at 200 °C for 10 mins. Then, the substrate was transferred into a glovebox. Perovskite active layer (20 mg mL^{-1}) was spin cast from toluene dispersions at 1000 rpm. LiF and Ag were then sequentially deposited by thermal evaporation in a vacuum deposition chamber (1×10^{-7} Torr).

Hole-only Device Fabrication. Cleaned ITO substrates were treated by UV-ozone for 20 mins. PEDOT: PSS (AI 4083) solution was spin-coated onto the ITO glass at 3000 rpm for 1 min and annealed in air at 150 °C for 15 mins. Then, the substrate was transferred into a glovebox. PNC active layer (20 mg mL^{-1}) was spin cast from

toluene dispersions at 1000 rpm. TCTA, MoO_3 and Ag were then sequentially deposited by thermal evaporation in a vacuum deposition chamber (1×10^{-7} Torr).

Device measurement. The current density-voltage (*J-V*) curves of the devices under diverse bias were measured by a Keithley 2400 sourcemeter. The LED brightness was determined using a Photo Research Spectra Scan spectrometer PR 655.

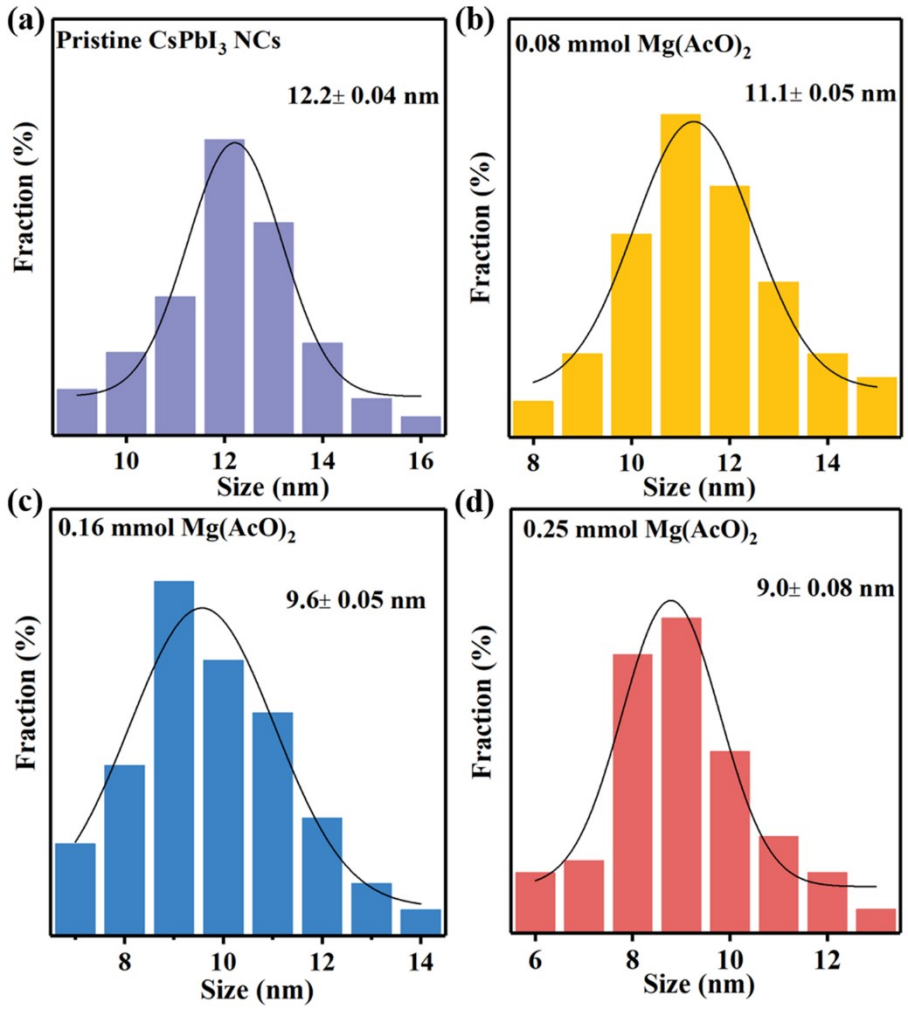

Figure S1. Diameter size distribution of (a) pristine $CsPbI_3$ NCs and (b) 0.08 mmol, (c) 0.16 mmol, (d) 0.25 mmol $Mg(AcO)_2$ modified $CsPbI_3$ NCs calculated from TEM images.

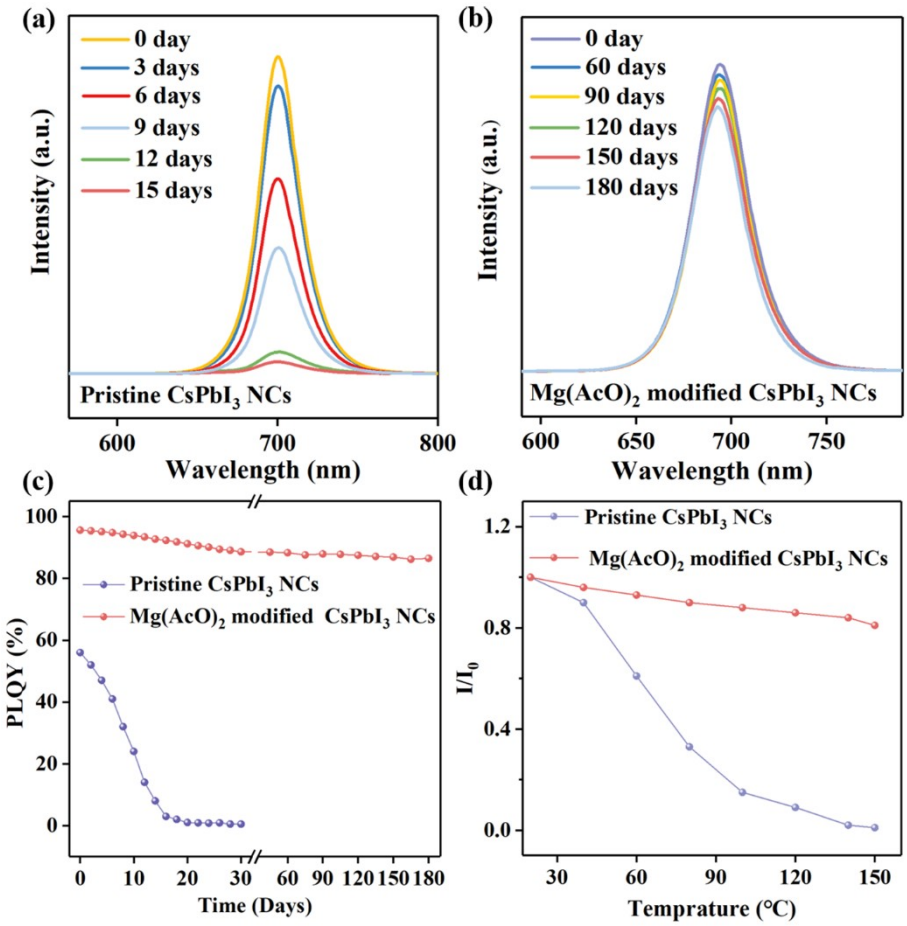

Figure S2. PL spectra of (a) pristine $CsPbI_3$ and (b) $Mg(AcO)_2$ modified $CsPbI_3$ NCs stored in ambient. (c) PLQY against storage time in ambient and (d) PL intensity versus temperature of the pristine $CsPbI_3$ NCs and $Mg(AcO)_2$ modified $CsPbI_3$ NCs.

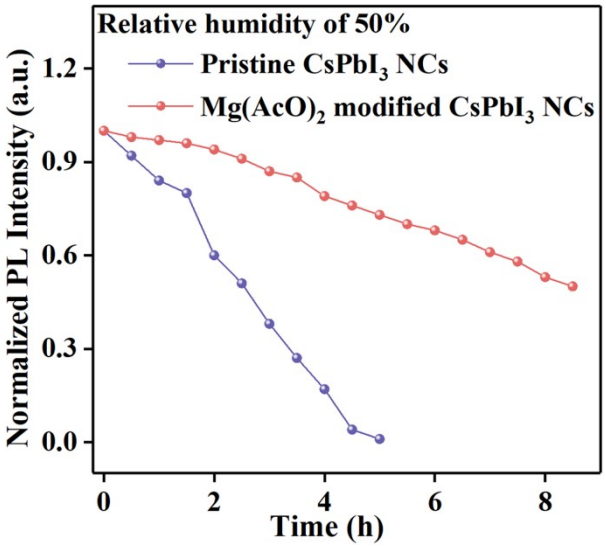

Figure S3. Comparison of the stability for the pristine $CsPbI_3$ NCs and $Mg(AcO)_2$ modified $CsPbI_3$ NCs under relative humidity of ≈50%.

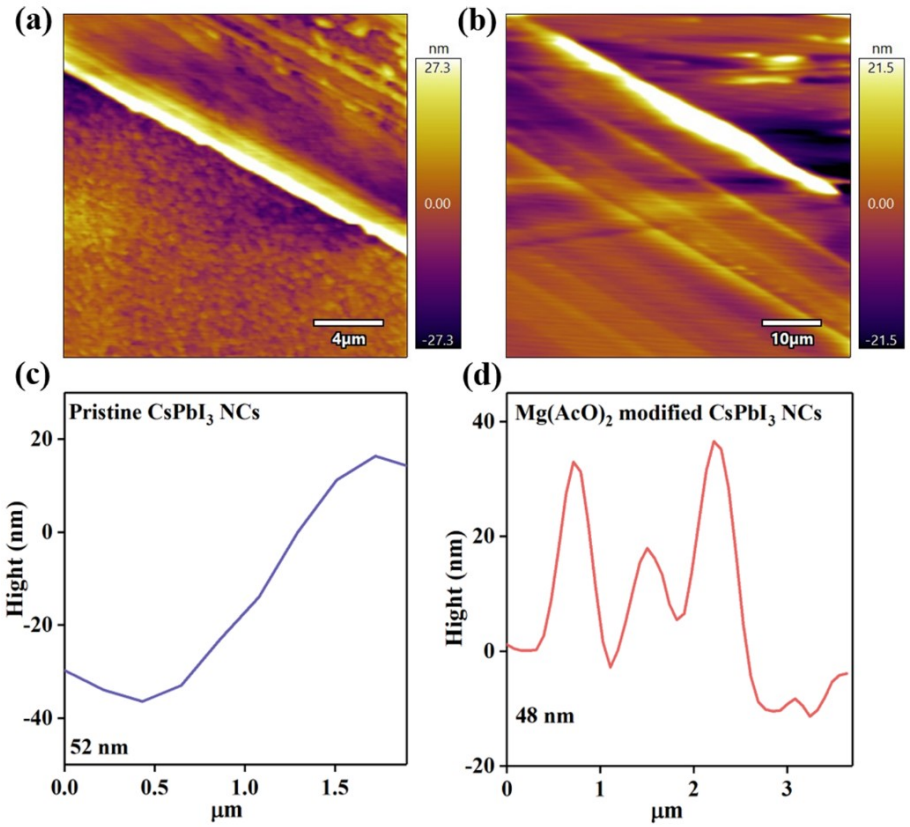

Figure S4. AFM characterization on thickness of perovskite NC film (a) pristine $CsPbI_3$ NCs and (b) after treatment with $Mg(AcO)_2$.

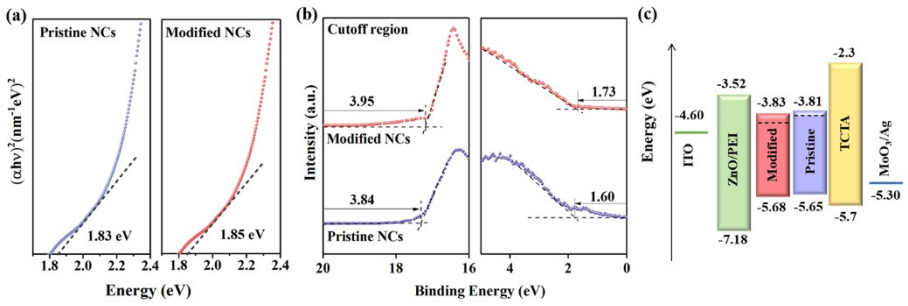

Figure S5. (a) Tauc plots, (b) UPS spectra and (c) energy levels of the functional layers in LED of pristine and modified $CsPbI_3$ NC films.

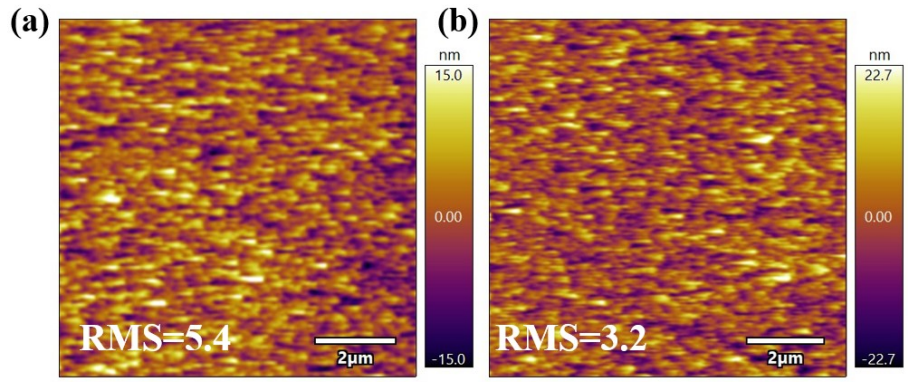

Figure S6. AFM images of (a) pristine and (b) modified $CsPbI_3$ NC films.

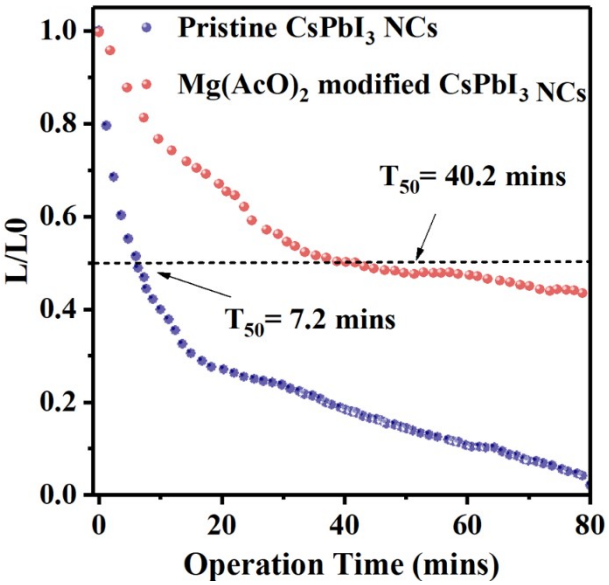

Figure S7. The operation stability of LEDs based on pristine and modified $CsPbI_3$ NCs.

Table S1. ICP of atomic ratio of Mg to Mg+Pb for $CsPbI_3$ NCs with adding different amount of $Mg(AcO)_2$.

$Mg(AcO)_2$ adding amounts (mmol)	0	0. 06	0.18	0.25
(ICP) atomic ratio of Mg/Mg+Pb (%)	0	2.1	10.4	16.1

Table S2. Data derived from the bi-exponential fitting of PL decay curves (τ_1,f_1, τ_2 and f_2), PL average lifetimes (τ_{avg}), radiative decay rates (k_r), PLQYs, and nonradiative decay rates (k_{nr}) of the pristine and the 0.25 mmol $Mg(AcO)_2$ modified $CsPbI_3$ NCs.

	Pristine $CsPbI_3$ NCs	$Mg(AcO)_2$ modified $CsPbI_3$ NCs
τ_1 (ns)	5.7	9.5
f_1 (%)	53.2	61.4
τ_2 (ns)	57.5	89.7
f_2 (%)	46.8	38.6
τ_{avg} (ns)	52.3	77.6
PLQY (%)	56.2	95.7
τ_r (ns)	93.5	90.9
τ_{nr} (ns)	119.0	181.8
K_r ($\times 10^6$ s^{-1})	10.7	11.0
K_{nr} ($\times 10^6$ s^{-1})	8.4	5.5

Table S3. Comparison of stability for the 0.25 mmol $Mg(AcO)_2$ modified $CsPbI_3$ NCs and the reported stability of the cubic $CsPbI_3$ NC without encapsulation.

Samples	Wavelength (nm)	PLQY (%)	Stability in ambient (day)	Thermal stability	Reference
$CsPbI_3$ NCs	680	99	110	-	1
$CsPbI_3$ NCs	687	93	30	PL intensity remains 87% after annealing at 117 ℃	2
$CsPbI_3$ NCs	680	95	100	-	3
$CsPbI_3$ NCs	689	99.8	70	-	4
$CsPbI_3$	680	100	160	-	5

NCs					
$CsPbI_3$ NCs	680	94	180	-	6
$CsPbI_3$ NCs	680	91	105	-	7
$CsPbI_3$ NCs	680	83	150	-	8
$CsPbI_3$ NCs	690	95.7	180	PL intensity remains 80% after annealing at 150 ℃	This work

Table S4. Resistance, thickness and conductivity of the films deposited from pristine $CsPbI_3$ NCs and 0.25 mmol $Mg(AcO)_2$ modified $CsPbI_3$ NCs. The resistances are determined from the slope of the *I-V* curves shown in Figure 5d in the maintext, thicknesses are measured by AFM characterization, and the conductivities are calculated fromthe formula: $\sigma = \frac{d}{AR}$.

Samples	Resistance (Ω)	Thickness (nm)	Conductivity (S/cm)
Pristine $CsPbI_3$ NCs	100.8	52	1.3×10^{-2}
0.25 mmol $Mg(AcO)_2$ modified $CsPbI_3$ NCs	40.2	48	3.0×10^{-2}

REFERENCES

1 Q. Zeng, X. Zhang, Q. Bing, Y. Xiong, F. Yang, H. Liu, J.-y. Liu, H. Zhang, W. Zheng, A. L. Rogach and B. Yang, *ACS Energy Lett.*, 2022, **7**, 1963-1970.

2 N. Ding, Y. Wu, W. Xu, J. Lyu, Y. Wang, L. Zi, L. Shao, R. Sun, N. Wang, S. Liu, D. Zhou, X. Bai, J. Zhou and H. Song, *Light Sci. Appl.*, 2022, **11**, 91.

3 M. Liu, N. Jiang, H. Huang, J. Lin, F. Huang, Y. Zheng and D. Chen, *Chem. Eng. J.*, 2021, **413**, 127547.

4 C. Chen, T. Xuan, W. Bai, T. Zhou, F. Huang, A. Xie, L. Wang and R.-J. Xie, *Nano Energy*, 2021, **85**, 106033.

5 C. Lee, Y. Shin, A. Villanueva-Antolí, S. Das Adhikari, J. Rodriguez-Pereira, J. M. Macak, C. A. Mesa, S. Giménez, S. J. Yoon, A. F. Gualdrón-Reyes and I. Mora-Seró, *Chem. Mater.*, 2021, **33**, 8745-8757.

6 K. Chen, Q. Zhong, W. Chen, B. Sang, Y. Wang, T. Yang, Y. Liu, Y. Zhang and H. Zhang, *Adv. Funct. Mater.*, 2019, **29**, 1900991.

7 Y. Cai, H. Wang, Y. Li, L. Wang, Y. Lv, X. Yang and R.-J. Xie, *Chem. Mater.*, 2019, **31**, 881-889.

8 S. Bera, D. Ghosh, A. Dutta, S. Bhattacharyya, S. Chakraborty and N. Pradhan, *ACS Energy Lett.*, 2019, **4**, 1364-1369.